PHYSICS OF PLASMAS VOLUME 8, NUMBER 6 JUNE 2001

On the importance of parallel heat conduction and magnetic geometry for multifaceted radiation from the edge (MARFE)

M. Z. Tokar
Institut für Plasmaphysik, Forschungszentrum Jülich GmbH, Association FZJ-Euratom, 52425, Jülich, Germany

(Received 25 January 2001; accepted 19 March 2001)

An importance of parallel heat conduction in plasma for formation of multifaceted radiation from the edge (MARFE) is assessed analytically by taking into account the magnetic geometry of the tokamak. It is demonstrated for circular nonconcentric due to Shafranov shift magnetic surfaces that toroidally symmetric perturbations of a MARFE-like structure with a maximum at the high-field side have the largest growth rate. Both the threshold and characteristic poloidal width of these perturbations depend essentially on plasma parallel heat conduction and geometric characteristics.
 [DOI: 10.1063/1.1372178]

I. INTRODUCTION

Multifaceted radiation from the edge (MARFE), a toroidally symmetric loop of cold dense and intensively radiating plasma at the tokamak edge near the inner wall,[1–3] is normally considered as a result of a thermal condensation instability. This instability was proposed initially[4,5] as a possible mechanism for the formation of stars of relatively small masses and develops due to characteristic dependence of the energy loss, e.g., due to radiation from impurities, on the plasma temperature and density.

In spite of a large number of publications on MARFE (see, e.g., Refs. 6–9) some important points have not been completely clarified. In particular, the relevance of parallel heat conduction in plasma to the onset conditions of MARFE was assessed from controversial points of view. From an analysis analogous to that given in Ref. 5, it was demonstrated in the first papers on MARFE (see, e.g., Ref. 10) that this process, which suppresses the instability through smoothing of temperature perturbations, should be significantly engaged in the definition of critical parameters. Later it was recognized,[7,8] however, that for perturbations with a zero parallel component of the wave vector, $k_\parallel$, conductive heat transport along field lines does not work. Such perturbations should start to grow first of all when, e.g., the plasma density is ramped up and, thus, they should provoke MARFE.

Up to now it has been difficult to record experimentally an initial stage of instabilities leading to MARFE. Therefore, one can judge about the modes, which cause this phenomenon, only from the structure of MARFE itself. Its toroidal symmetry implies $k_\parallel \approx 1/qR$, where q is the safety factor and R the major radius of the magnetic surface. Although this value is small in comparison with those characterizing, e.g., the radial extent of MARFE, one cannot simply put $k_\parallel = 0$ because of the huge level of parallel heat conductivity. It will be shown in the present paper that this contradiction between theoretical predictions and observations can be resolved by taking into account the magnetic geometry of the tokamak. Namely, the latter predetermines that not perturbations of zero $k_\parallel$ but toroidally symmetric ones of a MARFE-like structure, i.e., with a maximum at the high-field side, have the largest growth rate. Both the threshold and characteristic poloidal width of these perturbations depend essentially on the plasma parallel heat conductivity in a way different from previous predictions.

The role of magnetic geometry in MARFE formation have been assessed up to now mainly in numerical modeling. In Ref. 11 a poloidal inhomogeneity in the heat flux from the plasma core caused by the Shafranov shift of magnetic surfaces or the existence of an X point was imposed as a boundary condition. In numerical calculations this led to MARFE formation. In considerations performed later, similar results were obtained by a more consistent inclusion of proper metric coefficients in the transport equations (see, e.g., Refs. 7, 12). Although these results clearly demonstrate the importance of magnetic geometry for the phenomenon of MARFE, they do not provide a straightforward insight in what way this comes into play. An analytical consideration for the divertor geometry where MARFE is located near the X point was performed in Ref. 13. Because of the complexity of the metric coefficients used, the results obtained also cannot be easily interpreted. Besides, in divertor tokamaks MARFE develops normally after a detachment from divertor plates and it is questionable to consider this as a primary result of the thermal condensation instability on closed magnetic surfaces.

In other papers the effect of tokamak geometry was introduced indirectly, prescribing inhomogeneities in other parameters. In Ref. 14 it was demonstrated that unstable eigenmodes reveal a MARFE-like structure when a sufficiently strong poloidal dependence of the perpendicular plasma heat conductivity is adopted. It is widely believed that some instabilities being responsible for the anomalous transport of charged particles and energy are suppressed at the high-field side by a ''good'' curvature of the lines of force. It is, however, difficult to assess quantitatively the resulting poloidal variation in the transport coefficients and to prove that this fulfills the necessary requirements. Moreover, measurements of fluctuations show an increase in the level of turbulence at the inner edge shortly before the appearance of MARFE.[10] This can decrease the poloidal inhomogeneity in the anomalous transport.

Characteristic scales for the change of the plasma density, temperature, etc., in the equilibrium state have been introduced in Ref. 15 for a local analysis of instabilities. These scales, however, especially those characterizing the changes in the poloidal direction, vary strongly on magnetic surfaces (e.g., they are infinite at symmetry planes). This makes the problem nonlocal, which should influence the instability conditions significantly.

In the present paper, in order to get transparent analytical results, the simplest case of cylindrical magnetic surfaces slightly nonconcentric due to the Shafranov shift will be considered. In Sec. II, to clarify the physics, an idealized case of a homogeneous plasma in unperturbed stationary states assumed often in analytical considerations of MARFE will be discussed. It will be shown that in the presence of a shift the perturbations of a MARFE-like structure, i.e., with a maximum at the high-field side, have the largest growth rate γ. The parallel heat conductivity affects the level of γ and the characteristic poloidal width of these perturbations. In Sec. III it will be demonstrated that modes with a finite period in the toroidal directions have a smaller γ. The limit of small parallel heat conduction will be treated in Sec. IV. The effect on the instability threshold of poloidal inhomogeneity in the unperturbed equilibrium before MARFE will be investigated in Sec. V.

II. TOROIDALLY SYMMETRIC PERTURBATIONS IN HOMOGENEOUS STATIONARY PLASMA

In this section small perturbations of stationary homogeneous nonflowing edge plasma will be considered. They are described by the set of linearized two-dimensional 2-D equations for the transport of charged particles, their parallel momentum, and energy:[16]

$$\frac{\partial \tilde{n}}{\partial t}+n\frac{\partial \tilde{V}}{\partial l}=0, \tag{1}$$

$$mn\frac{\partial \tilde{V}}{\partial t}+2\frac{\partial \widetilde{nT}}{\partial l}=0, \tag{2}$$

$$3\frac{\partial \widetilde{nT}}{\partial t}+\nabla_\perp \tilde{q}_\perp+\frac{\partial}{\partial l}\left(-\kappa_\parallel\frac{\partial \tilde{T}}{\partial l}+5nT\tilde{V}\right)=-\tilde{Q}_{\text{rad}}. \tag{3}$$

Here n, $\tilde{n}$, T, and $\tilde{T}$ are stationary values and perturbations of the plasma density and temperature are assumed to be the same for electrons and the main ions of the mass m; $\tilde{V}$ the parallel (along the direction l) plasma velocity in the perturbed state; $q_\perp$ the density of the heat flux perpendicular to the magnetic surfaces, and $\kappa_\parallel$ the parallel electron heat conductivity. Here Q_{rad} is the power density of radiation losses; this depends on n and T and

$$\tilde{Q}_{\text{rad}}=Q_{\text{rad}}\left(\sigma_n\frac{\tilde{n}}{n}+\sigma_T\frac{\overline{T}}{T}\right),$$

with $\sigma_T=d\ln Q_{\text{rad}}/d\ln T$ and $\sigma_n=d\ln Q_{\text{rad}}/d\ln n$, which are assumed given. Terms that account for sources and transport of charged particles and their momentum perpendicular to the magnetic field are omitted in Eqs. (1)–(3) in order to avoid any complexity unimportant for the subject of the present paper.

Equations (1) and (2) are combined as follows:

$$m\frac{\partial^2 \tilde{n}}{\partial t^2}=2\frac{\partial^2 \widetilde{nT}}{\partial l^2}.$$

As it has been shown in Ref. 5, the condensation mode is aperiodic, i.e., a small perturbation of stationary plasma parameters varies in time as $\exp(\gamma t)$ with a real growth rate γ. The left-hand side of the latter equation is proportional to γ^2 and, in the vicinity of the instability threshold where $\gamma\to 0$, the variations of the plasma density and temperature do not change its pressure nT and $\tilde{n}/n=-\tilde{T}/T$.

For toroidally symmetric perturbations $\partial l=qR\partial\vartheta$, where ϑ is the poloidal angle and $\vartheta=0$ corresponds to the high-field side. Henceforth, ϑ and the difference x between the minor radii of the last closed magnetic surface (LCMS) and the considered one will be used as independent variables. Equation (1) allows one to exclude convective energy flow from Eq. (3) and, by taking the pressure constancy into account, this equation is rewritten as follows (see Appendix):

$$5n\frac{\partial \tilde{T}}{\partial t}-g^{xx}\kappa_\perp\frac{\partial^2 \tilde{T}}{\partial x^2}-\frac{\kappa_\parallel}{(qR)^2}\frac{\partial^2 \tilde{T}}{\partial \vartheta^2}=Q_{\text{rad}}(\sigma_T-\sigma_n)\frac{\tilde{T}}{T}, \tag{4}$$

where $\kappa_\perp$ is the perpendicular plasma heat conductivity and the metric coefficient,

$$g^{xx}\approx 1-\Delta_1\cos\vartheta,$$

with $\Delta_1=2(d\Delta/dx)>0$ accounts for Shafranov shift Δ of magnetic surfaces.

Consider perturbations of some wave vector $k_\perp$ perpendicular to the magnetic surfaces. The solutions of Eq. (4) can be looked for in the form $\tilde{T}=\Theta(\vartheta)\times\exp(\gamma t+ik_\perp x)$. Substituting this in Eq. (4), one gets an equation for the function Θ:

$$\frac{d^2\Theta}{d\vartheta^2}=\frac{(qR)^2}{\kappa_\parallel}\left[\frac{Q_{\text{rad}}}{T}(\sigma_T-\sigma_n)+(1-\Delta_1\cos\vartheta)\kappa_\perp k_\perp^2+5n\gamma\right]\Theta. \tag{5}$$

By changing the independent variable, $z=1/2(\pi-\theta)$, Eq. (5) is reduced to a canonical form of Mathieu's equation:[17]

$$\frac{d^2\Theta}{dz^2}+[a-2p\cos(2z)]\times\Theta=0, \tag{6}$$

with the coefficients

$$a=-\frac{(2qR)^2}{\kappa_\parallel}\left[\frac{Q_{\text{rad}}}{T}(\sigma_T-\sigma_n)+\kappa_\perp k_\perp^2+5n\gamma\right] \tag{7}$$

and

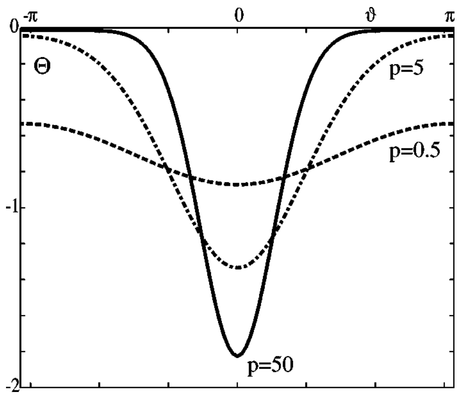

FIG. 1. Poloidal shape of toroidally symmetric temperature perturbations described by Mathieu's function of zero order.

$$p=\frac{2(qR)^2}{\kappa_\parallel}k_\perp^2\kappa_\perp\Delta_1. \tag{8}$$

Periodic solutions of Mathieu's equation exist for a countable infinite set of characteristic values $a_l(p)$. As functions of z they have period π or 2π. Only those of period π are of interest for us because they are functions of period 2π with respect to the poloidal angle ϑ. This restricts the class of functions in question to $ce_{2m}[z=(\pi-\theta)/2,p]$ with $m=0,1,2,...$, and $se_{2m}[z=(\pi-\theta)/2,p]$ with $m=1,2,...$. It is shown in Ref. 17 that for any p the lowest a and, thus the highest γ, are provided by the even Mathieu's functions of the zeroth order, ce_0. These functions are shown in Fig. 1 for different p. With increasing p, i.e., increasing Δ_1 or decreasing $\kappa_\parallel$, the ϑ dependence of ce_0 reveals a MARFE-like structure more and more clearly. As an example, consider the onset of MARFE in the tokamak experiment for technology oriented research (TEXTOR).[18] For typical plasma parameters at the inner edge,[18] $q=3.7$, $R=175$ cm, $k_\perp=1\ \mathrm{cm}^{-1}$, $\kappa_\perp=10^{18}\ \mathrm{cm}^{-1}\,\mathrm{s}^{-1}$, $T\approx 15$ eV, i.e., $\kappa_\parallel\approx 4\times 10^{22}\ \mathrm{cm}^{-1}\,\mathrm{s}^{-1}$, and $\Delta_1\approx 0.5$, we get $p\approx 20$. During a nonlinear development of perturbations, $\kappa_\parallel$ decreases with the plasma temperature as $T^{2.5}$, which leads to a brighter manifestation of the MARFE structure. An analysis of nonlinear evolution will be done elsewhere.

For small p it holds[17] $a_0\approx-\frac{1}{2}p^2$, and one gets

$$\gamma=\gamma_0+\frac{q^2R^2}{\kappa_\parallel}\frac{(k_\perp^2\kappa_\perp\Delta_1)^2}{10n}, \tag{9}$$

where

$$\gamma_0=\frac{1}{5n}\left(\frac{Q_{\mathrm{rad}}}{T}(\sigma_n-\sigma_T)-\kappa_\perp k_\perp^2\right) \tag{10}$$

is the growth rate of perturbations homogeneous on the magnetic surfaces in the case without Shafranov shift.[8] In the presence of a finite shift the perturbations described by Mathieu's functions ce_0 have the growth rate larger than γ_0. The critical level of the energy losses follows from the condition $\gamma=0$:

$$Q_{\mathrm{rad}}^{\mathrm{cr}}=\frac{\kappa_\perp k_\perp^2 T}{\sigma_n-\sigma_T}\left(1-(qRk_\perp\Delta_1)^2\frac{\kappa_\perp}{2\kappa_\parallel}\right). \tag{11}$$

It is of importance to compare Eq. (9) with predictions of previous analyses for the growth rate of modes with a given parallel wave number $k_\parallel$ (see, e.g., Refs. 6–8, 10):

$$\gamma=\gamma_0-\frac{\kappa_\parallel k_\parallel^2}{5n}. \tag{12}$$

By making the substitution of $1/k_\parallel^2$ instead of q^2R^2 we obtain from Eq. (9),

$$\gamma=\gamma_0+\frac{1}{\kappa_\parallel k_\parallel^2}\frac{(k_\perp^2\kappa_\perp\Delta_1)^2}{10n}. \tag{13}$$

In principal agreement with Eq. (12), this formula predicts that the growth rate decreases with increasing $k_\parallel$, i.e., higher $k_\parallel$ modes are more stable than lower $k_\parallel$ modes. This is predetermined by the intrinsic stabilizing nature of heat conduction. However, perturbations given by Mathieu's functions contain a infinite number of harmonics, including the one with the lowest $k_\parallel=0$:[17]

$$ce_0=\frac{1}{\sqrt{2}}\left[1-\frac{p}{2}\cos 2z+p^2\left(\frac{\cos 4z}{32}-\frac{1}{16}\right)+\cdots\right]$$
$$=\frac{1}{\sqrt{2}}\left[1+\frac{p}{2}\cos\vartheta+p^2\left(\frac{\cos 2\vartheta}{32}-\frac{1}{16}\right)+\cdots\right]. \tag{14}$$

Therefore, relations for a single $k_\parallel$ cannot explain all features of Eq. (9). In particular, this formula predicts that the stabilizing effect of heat conduction saturates with increasing $\kappa_\parallel$. Physically this is explained as follows: the larger $\kappa_\parallel$ the smoother the temperature perturbation on the magnetic surface. Mathematically, one can see this from the above expansion for ce_0, predicting that with increasing $\kappa_\parallel$ the weight of harmonics with $k_\parallel\neq 0$ becomes smaller because p decreases as $1/\kappa_\parallel$. Therefore the growth rate of perturbations given by ce_0 should approach to γ for poloidally homogeneous modes, for which the parallel heat transport does not work. This approaching of γ to γ_0 with increasing $\kappa_\parallel$ is prescribed by Eq. (9). Equation (12), derived for single Fourier modes, which are not eigenfunctions in plasmas with a finite Shafranov shift, cannot mimic this variation of relative contributions from different $k_\parallel$ with changing parallel heat conduction.

It is also instructive to note that axissymmetry of the perturbations, for which Eq. (9) has been derived, is a key point for their evolution with increasing $\kappa_\parallel$. For perturbations with a finite toroidal wavelength, the case considered in the next section, the term $-\kappa_\parallel k_\varphi^2$ recovers [see Eq. (15)] and provides a higher stability.

In the opposite limit of $\kappa_\parallel\to 0$, Eq. (12) predicts no effect of parallel heat transport on the MARFE onset. Equation (9) cannot be, however, applied in this case because the approximation of small p does not hold. This situation will be analyzed in Sec. IV and it will be shown that our approach also predicts the vanishing effect of $\kappa_\parallel$. Nevertheless, the influence of geometry does not disappear at all because the critical parameters are determined in this case by the perpendicular heat conduction at $\vartheta=0$, where this transport channel is the weakest.

III. TOROIDALLY PERIODIC PERTURBATIONS

In this section we intend to demonstrate that a distortion of the axisymmetry of the perturbations results in a reduction of their growth rate. For the case of a finite Shafranov shift it makes no sense to analyze perturbations constant along field lines: as the perturbations constant on magnetic surfaces they are not eigenfunctions of the system with finite Δ and cannot be excited spontaneously. Therefore, we consider more general perturbations that have a finite wave length in the toroidal direction without prescribing their poloidal structure *a priori*. Due to continuity of the plasma parameters these perturbations should be periodic functions of the toroidal angle φ. In a stationary state our system is axisymmetric and such perturbations can be represented by uncoupled harmonics $e^{im\varphi}$ with integer m. In this case, the divergence of the parallel heat flux in Eq. (5) should be supplemented with the term $-(\kappa_\parallel/R^2)[(2im/q)(\partial\Theta/\partial\vartheta)-m^2\Theta]$. The resulting equation is multiplied by Θ and integrated over ϑ from 0 to 2π. Then, by taking into account the continuity of Θ and $\partial\Theta/\partial\vartheta$, we get for the growth rate,

$$\gamma_{m\neq 0}=\gamma_0-\frac{\kappa_\parallel}{5n}\left(k_\varphi^2+\frac{\xi_1}{q^2R^2}\right)+\frac{\kappa_\perp\Delta_1 k_\perp^2}{5n}\xi_2, \tag{15}$$

where

$$k_\varphi=\frac{m}{R},\quad \xi_1=\frac{\int_0^{2\pi}\left(\frac{\partial\Theta}{\partial\vartheta}\right)^2 d\vartheta}{\int_0^{2\pi}\Theta^2 d\vartheta},\quad \xi_2=\frac{\int_0^{2\pi}\Theta^2\cos\vartheta\, d\vartheta}{\int_0^{2\pi}\Theta^2 d\vartheta}.$$

Since $\xi_1\geqslant 0$ and $\xi_2\leqslant 1$, one has

$$\gamma_{m\neq 0}\leqslant\gamma_0-\frac{\kappa_\parallel k_\varphi^2}{5n}+\frac{\kappa_\perp\Delta_1 k_\perp^2}{5n}$$

or

$$\gamma_{m\neq 0}\leqslant\gamma-\frac{\kappa_\parallel}{5nR^2}\left(m^2-\zeta+\frac{q^2}{2}\zeta^2\right),$$

with $\zeta=\kappa_\perp\Delta_1 k_\perp^2 R^2/\kappa_\parallel$. As a function of ζ, the right-hand side of the inequality above has a maximum, and computing this we come to the condition

$$\gamma_{m\neq 0}\leqslant\gamma-\frac{\kappa_\parallel}{5nR^2}\left(m^2-\frac{1}{2q^2}\right). \tag{16}$$

Since at the plasma edge $q>1$, this condition implies that toroidally symmetric perturbations always have a growth rate larger than that of perturbations with a finite toroidal period. This is preconditioned by a large toroidal temperature gradient produced by the latter, which leads to a stronger suppressive effect from parallel heat transport. Conversely, the MARFE-like toroidally symmetric perturbations organize themselves in such a way that their stabilization by parallel heat conduction is minimal.

IV. LIMIT OF SMALL PARALLEL HEAT CONDUCTIVITY

For a sufficiently large Δ_1 or small $\kappa_\parallel$, Eq. (11) predicts that $Q_{\mathrm{rad}}^{\mathrm{cr}}$ reduces to zero. However, this is not realized because the approximate quadratic dependence of a_0 vs p assumed above does not hold for $p\gtrsim 1$ and the asymptotic relation $a_0\approx -2p$ can be used for $p\gg 1$. One can see that, in this case, the parallel heat conductivity falls out from the expression for γ and

$$Q_{\mathrm{rad}}^{\mathrm{cr}}=\kappa_\perp k_\perp^2 T\frac{1-\Delta_1}{\sigma_n-\sigma_T}. \tag{17}$$

This formally coincides with the local critical value of Q_{rad} at $\vartheta=0$, which follows from Eq. (5) when the parallel heat transport is neglected and different poloidal positions are decoupled. In this case, it follows from Eq. (5) that $\gamma<0$ for $\vartheta\neq 0$. This means a zero width of the unstable region in the poloidal direction, which agrees with the vanishing characteristic width of the Mathieu's function ce_0 when $p\to\infty$. Qualitatively, this can be explained as follows: with $\kappa_\parallel\to 0$ the MARFE threshold corresponds to the threshold of a local radial detachment at the position of the smallest $g^{xx}(\vartheta)$, i.e., where the distance between magnetic surfaces is the largest and the stabilizing perpendicular transport of heat is the weakest one.

V. INSTABILITY OF REALISTIC INHOMOGENEOUS EQUILIBRIUM

In reality, a stationary equilibrium state without MARFE is already not completely poloidally symmetric in the presence of a Shafranov shift. Through the temperature dependence in Q_{rad} and $\kappa_\parallel$, this influences the critical parameters for the development of instabilities leading to MARFE. An exact determination of the two-dimensional temperature profile at the plasma edge requires a numerical solution of the heat transport equation and is out of the scope of the present consideration. Here we confine ourselves to an approximate approach to assess the role of the poloidal inhomogeneity of the equilibrium state. Only the temperature variation at the (LCMS) is considered. Here the divergence of the perpendicular heat flux is approximated as follows:

$$\frac{\partial}{\partial x}\left(\kappa_\perp\frac{\partial T}{\partial x}\right)\approx\frac{q_{\mathrm{core}}-q_{\mathrm{LCMS}}}{x_{\mathrm{rad}}}, \tag{18}$$

where q_{core} and q_{LCMS} are the densities of the heat flux from the plasma core and through the LCMS, respectively, and x_{rad} the width of the radiative layer. The q_{core} is determined by the input power and q_{LCMS} is controlled by the temperature at the LCMS itself through the e-folding length in the scrape-off layer, $\delta_T: q_{\mathrm{LCMS}}=\kappa_\perp T(x=0)/\delta_T$. Both δ_T and x_{rad} are normally of several cm.

Under the condition $\Delta_1\ll 1$, the poloidal dependence of the temperature in an equilibrium state without MARFE can be looked for as follows:

$$T(x=0,\vartheta)\approx T_0+T_1\cos\vartheta. \tag{19}$$

Substituting this representation in a stationary heat balance equation, one finds the coefficients $T_{0,1}$:

$$T_0\approx\delta_T\frac{q_{\mathrm{core}}-Q_{\mathrm{rad}}x_{\mathrm{rad}}}{\kappa_\perp}, \tag{20}$$

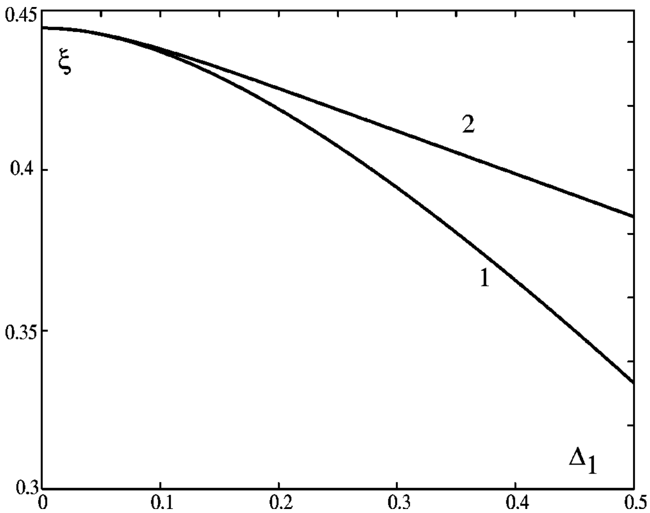

FIG. 2. Critical for MARFE development level of radiation losses, $\xi = Q_{\rm rad}^{\rm cr}/\kappa_\perp \kappa_\perp^2 T_0$ vs the derivative of the the Shafranov shift for idealized homogeneous (1) and poloidally asymmetric given by Eqs. (19)–(21) equilibria (2).

$$T_1 \approx -T_0 \times \frac{\Delta_1}{\sigma_T - \sigma_n + \dfrac{T_0}{Q_{\rm rad}}\left(\dfrac{\kappa_\parallel}{q^2R^2} + \dfrac{\kappa_\perp}{\delta_T x_{\rm rad}}\right)}. \tag{21}$$

If the poloidal inhomogeneity in stationary temperature and density (through pressure balance) is taken into account in coefficients of Eq. (3), one gets Eq. (6) for $\widetilde{T^{1+\beta}}$ with a modified coefficient p:

$$p = \frac{2q^2R^2}{\kappa_\parallel}\left[\kappa_\perp k_\perp^2\left(\Delta_1 + \beta\frac{T_1}{T_0}\right) + \beta\frac{T_1}{T_0}\left(Q_{\rm rad}\frac{\sigma_T - \sigma_n}{T_0} + 5\gamma n\frac{1+\beta}{\beta}\right)\right], \tag{22}$$

where $\beta = 2.5$ stems from the temperature dependence of $\kappa_\parallel$.

With an accuracy of 10% the asymptotic relations between a_0 and p used in the sections above are conjugated by the formula $a_0 \approx -2p^2/(4+p)$. At the instability threshold, $\gamma = 0$, this provides a transcendental equation for the critical level of radiation losses, $Q_{\rm rad}^{\rm cr}$. Figure 2 presents the numerically found dependence of $\xi = Q_{\rm rad}^{\rm cr}/\kappa_\perp k_\perp^2 T_0$ on the parameter Δ_1 for $\beta = 0$, which reproduces the case of poloidally homogeneous equilibrium discussed above, and for $\beta = 2.5$. For $\Delta_1 \ll 1$, when both the equilibrium and perturbed states are very weakly influenced by the Shafranov shift, both curves coincide. With increasing Δ_1, the effect of the inhomogeneity in the equilibrium caused by the shift becomes significant and the tendency can be explained as follows. The increase of the distance between neighboring magnetic surfaces at the inner edge, $\vartheta = 0$, with respect to the poloidally averaged level [the first term in the first round brackets in Eq. (22)] is partly compensated for by the enhanced temperature difference between surfaces caused by the poloidal inhomogeneity in the temperature profile (the second term in these brackets). This effect even exceeds the increase of the radiation losses with decreasing temperature at the inner edge (the first term in the second round brackets). Therefore, the asymmetry in the radial heat flux decreases and an instability develops at a higher radiation level.

VI. CONCLUSION

The peculiarities of magnetic geometry in tokamaks predetermines the importance of parallel heat conduction for MARFE development. This has been proven for the case of circular nonconcentric due to Shafranov shift magnetic surfaces, where the MARFE-like toroidally symmetric perturbations described by even Mathieu's functions of the zero order have the largest growth rate. The parallel heat conductivity of the plasma controls both the growth rate and the characteristic width of these perturbations. However, in distinction to the earlier predictions, the effect of $\kappa_\parallel$ reduces as this becomes large because temperature perturbations become smoother on magnetic surfaces and their stability is determined only by the perpendicular heat transport. In the opposite limit of small $\kappa_\parallel$, different poloidal positions are decoupled and the MARFE threshold coincides with the threshold of a local radial detachment at the high-field side where the perpendicular transport is minimal. The poloidal inhomogeneity in the equilibrium temperature profile leads to a weaker dependence of the MARFE threshold on the Shafranov shift.

An analogous consideration of the linear stage of MARFE formation in a divertor configuration is more complicated due to, at least, two factors: (i) the energy sink to the divertor plates should be included, (ii) the metric coefficients in the vicinity of the X point are too complex for a transparent analytical analysis. Nevertheless, the result of the present study allows one to state qualitatively the following: the position of the final MARFE near the X point is predetermined by the largest distance between neighboring magnetic surfaces and thus the weakest perpendicular heat transport, and the poloidal dimension of MARFE is governed by the level of the parallel heat conduction.

APPENDIX

In an arbitrary coordinate system, the divergence of the density of conductive heat flux can be written as follows:[19]

$$\nabla \vec{q} = \frac{1}{\sqrt{g}}\frac{\partial}{\partial x^i}\left(-\sqrt{g}\,\frac{\kappa_{jk}}{g_{ik}}\frac{\partial T}{\partial x^j}\right),$$

where g is the discriminant of the metric tensor whose components, g_{ik}, determine the square of the element of length: $(dl)^2 = \Sigma g_{ik} dx^i dx^k$. It is assumed that only the transport across circular nonconcentric magnetic surfaces and along the lines of force contribute to the heat conduction tensor κ_{jk}. In such a case, it is convenient to introduce a coordinate system $x^1 = x \equiv a - r$, $x^2 = \vartheta$, and $x^3 = \varphi$, where r is the minor radius of the magnetic surface, ϑ and φ are the poloidal and toroidal angles, respectively; a and R_0 are the minor and major radii of the last closed magnetic surface.

In a cylindrical coordinate system with the radial coordinate R, toroidal angle φ, and vertical axis Z, which coincides with the axis of tokamak, the magnetic surface of the minor radius r is described by the equations

$$R=R_0+\Delta-r\times\cos\vartheta,\quad Z=r\times\sin\vartheta,$$

where $\Delta(r)$ is the Shafranov shift of the surface center. Since $(dl)^2=(dR)^2+(Rd\varphi)^2+(dZ)^2$ one gets easily the metric coefficients in the coordinate x, ϑ, φ. With an accuracy up to linear terms with respect to Δ,

$$g_{xx}=1+2\cos\vartheta\frac{d\Delta}{dx},$$

$$g_{x\vartheta}=g_{\vartheta x}=(x-a)\frac{d\Delta}{dx}\sin\vartheta,$$

$$g_{\vartheta\vartheta}=(a-x)^2,\quad g_{\varphi\varphi}=R^2,$$

$$g_{x\varphi}=g_{\varphi x}=g_{\vartheta\varphi}=g_{\varphi\vartheta}=0.$$

By taking into account that $\partial/\partial l=(B_\vartheta/B)(1/r)(\partial/\partial\vartheta)+(B_\varphi/B)(1/R)(\partial/\partial\varphi)\approx(1/qR)(\partial/\partial\vartheta)+(1/R)(\partial/\partial\varphi)$, we obtain

$$\nabla\vec{q}=\frac{1}{\sqrt{g}}\frac{\partial}{\partial x}\left(-\sqrt{g}\frac{\kappa_\perp}{g_{xx}}\frac{\partial T}{\partial x}\right)+\frac{1}{\sqrt{g}R^2}\left(\frac{1}{q}\frac{\partial}{\partial\vartheta}+\frac{\partial}{\partial\varphi}\right)\times\left[-\sqrt{g}\kappa_\parallel\left(\frac{1}{q}\frac{\partial T}{\partial\vartheta}+\frac{\partial T}{\partial\vartheta}\right)\right].$$

For axisymmetric perturbations and under the assumption that $d\Delta/dx\ll 1$ and q varies weakly in the edge region where $x\ll a$, one gets

$$\nabla\vec{q}\approx g^{xx}\frac{\partial}{\partial x}\left(-\kappa_\perp\frac{\partial T}{\partial x}\right)+\frac{1}{q^2R^2}\frac{\partial}{\partial\vartheta}\left(-\kappa_\parallel\frac{\partial T}{\partial\vartheta}\right)+\frac{\kappa_\parallel\sin\vartheta}{\sqrt{g}q^2R^2}\frac{\partial T}{\partial\vartheta}\frac{d\Delta}{dx},$$

with $g^{xx}\approx 1-2(d\Delta/dx)\cos\vartheta$. The poloidal inhomogeneity in temperature is caused by the Shafranov shift, i.e., $\partial T/\partial\vartheta\sim d\Delta/dx$. Thus, the last term in the above expression is of the second order with respect to $d\Delta/dx$ and can be neglected in the first approximation.

[1] J. L. Terry, E. S. Marmar, S. M. Wolfe *et al.*, Bull. Am. Phys. Soc. **26**, 886 (1981).
[2] F. Alladio, R. Bartiromo, B. Casali *et al.*, Phys. Lett. A **90**, 405 (1982).
[3] D. R. Baker, R. T. Snider, and M. Nagami, Nucl. Fusion **22**, 807 (1982).
[4] E. N. Parker, Astrophys. J. **117**, 431 (1953).
[5] G. B. Field, Astrophys. J. **142**, 531 (1965).
[6] J. F. Drake, Phys. Fluids **30**, 2429 (1987).
[7] A. De Ploey, R. A. M. Van der Linden, G. T. A. Huysmans, M. Goossens, W. Kerner, and J. P. Goedbloed, Plasma Phys. Controlled Fusion **39**, 423 (1997).
[8] W. M. Stacey, Plasma Phys. Controlled Fusion **39**, 1245 (1997).
[9] P. C. Georgiou, M. G. Haines, and R. J. Hastie, Contrib. Plasma Phys. **38**, 136 (1998).
[10] B. Lipschultz, B. LaBombard, E. S. Marmar, M. M. Pickrell, J. L. Terry, R. Watterson, and S. M. Wolfe, Nucl. Fusion **24**, 977 (1984).
[11] J. Neuhauser, W. Schneider, and R. Wunderlich, Nucl. Fusion **26**, 1679 (1986).
[12] H. Kastelewicz, R. Schneider, and J. Neuhauser, Plasma Phys. Controlled Fusion **37**, 723 (1995).
[13] Yu. Igithanov and M. Mikhailov, J. Nucl. Mater. **266–269**, 837 (1999).
[14] R. Singh, C. V. S. Rao, K. Avinash, S. P. Deshpande, and P. K. Kaw, Nucl. Fusion **32**, 379 (1992).
[15] W. M. Stacey, Phys. Plasmas **3**, 3032 (1996).
[16] S. I. Braginski, in *Reviews of Plasma Physics*, edited by M. Leontovich (Consultants Bureau, New York, 1963), Vol. 1, p. 193.
[17] *Handbook of Mathematical Functions*, edited by M. Abramowitz and I. A. Stegun, 9th ed. (Dover, New York, 1970), p. 722.
[18] J. Rapp, P. C. DeVries, F. C. Schüller *et al.*, Nucl. Fusion **39**, 765 (1999).
[19] R. Balescu, *Transport Processes in Plasmas* (North Holland, Amsterdam, 1988), Vol. 2, p. 246.